

Alignment of velocity and vorticity and the intermittent distribution of helicity in isotropic turbulence

Yeontaek Choi,^{*} Byung-Gu Kim, and Changhoon Lee[†]

*Department of Mechanical Engineering and Department of Computational Science and Engineering,
Yonsei University, 134 Shinchon-dong, Seodaemun-gu, Seoul 120-749, Korea*

(Received 24 May 2008; revised manuscript received 5 February 2009; published 22 July 2009)

We provide an observation suggesting a strong correlation between helicity and enstrophy in fluid turbulence. Helicity statistics were obtained in a direct numerical simulation of forced isotropic turbulence. An investigation of coherent structures revealed that intermittently large local helicity was found in the core region of the coherent rotational structures, thus showing a strong correlation with local enstrophy, not dissipation. Statistics regarding the relative helicity and the correlation between velocity and vorticity conditioned on different levels of enstrophy clearly suggest that velocity and vorticity tend to be aligned in the core of the coherent structures.

DOI: [10.1103/PhysRevE.80.017301](https://doi.org/10.1103/PhysRevE.80.017301)

PACS number(s): 47.27.Gs, 47.27.ek, 47.27.De

Local helicity H , defined by $H = \mathbf{u} \cdot \boldsymbol{\omega}$, where \mathbf{u} is velocity and $\boldsymbol{\omega}$ is vorticity, has been known to play an important role in the evolution and stability of laminar and turbulent flows [1]. In particular, several aspects of the role of helicity in turbulent flows have been investigated, including the helicity cascade [2–8], helicity spectra and dissipation [9–13], the helical nature of coherent structures [14–17], and even the pure mathematics [18].

The intermittent distribution of local helicity is an interesting phenomenon in fluid turbulence. Intermittency of local helicity can be studied in two contexts. First, helicity has some connection with nonlinear energy transfer, represented by $\mathbf{u} \times \boldsymbol{\omega}$, which naturally involves energy dissipation which is also an intermittent quantity. Helicity has a function to depress the nonlinear energy-transfer process [19–26]. This can be understood via the rotational form of the Navier-Stokes equations, $\frac{\partial \mathbf{u}}{\partial t} + \mathbf{u} \times \boldsymbol{\omega} = -\nabla(\frac{p}{\rho} + \frac{1}{2}u^2) + \nu \Delta \mathbf{u}$, and a trigonometric identity, $(\mathbf{u} \times \boldsymbol{\omega})^2 / (|\mathbf{u}|^2 |\boldsymbol{\omega}|^2) + (\mathbf{u} \cdot \boldsymbol{\omega})^2 / (|\mathbf{u}|^2 |\boldsymbol{\omega}|^2) = 1$, showing that when velocity and vorticity are parallel with each other, nonlinear energy transfer is prohibited. This is consistent with a previous observation that regions which are predominantly occupied by $\mathbf{u} \times \boldsymbol{\omega}$ and $\mathbf{u} \cdot \boldsymbol{\omega}$ do not overlap each other [16].

Alternately, helicity can be investigated in connection with local enstrophy, which is another intermittent quantity. Local helicity distributed on the turbulent structures has some nontrivial correlations with local enstrophy [14–16,27]. Given that helicity is an interaction between the velocity and vorticity vectors and the interaction is fully manifested on the turbulent structures, it is natural to examine the relation between local helicity and local enstrophy.

The aim of this Brief Report is to explain the cause of the intermittency of helicity in relation to coherent vortical structures. Similar approaches to explain the intermittencies of enstrophy and dissipation in connection with vortical structures have been reported [28–30]. In our study, distinctive

correlations between helicity and enstrophy will be suggested. Also, the alignment between velocity and vorticity vectors is investigated near the vortical structures.

The calculations performed in this Brief Report were obtained by direct numerical simulations. The governing equations, including the Navier-Stokes equation and the continuity equation, were solved by employing a spectral method for spatial discretization and the third-order Runge-Kutta scheme for time advancement in a $(2\pi)^3$ cubic domain. Most calculations were carried out with 64^3 and 128^3 grid numbers and the resulting R_λ are around 46 and 87, respectively. Results with 64^3 grids were not reported in this Brief Report, but were only briefly stated for comparison to the calculations with 128^3 grids. For the maintenance of stationarity, we used the forcing scheme proposed by Eswaran and Pope [31] so that the artificially forced low-wave-number velocity components generate statistically stationary turbulence fields. This forcing scheme produces zero mean helicity, but nonzero local helicity.

It is important to briefly mention the influence of the large-scale forcing. It is well known that large-scale forcing can strongly influence small-scale structures in relatively low Reynolds number calculations. However, as pointed out in the previous studies [31–37], the effects presented by the large-scale forcing calculated in similar situations to our calculations are either negligible or not as strong. The results for 64^3 grid size with a R_λ around 45 would produce more forcing-dependent property, but they exhibited similar results to the calculation for 128^3 and $R_\lambda = 87$: all statistics such as energy spectrum, probability distributions of enstrophy, energy dissipation, helicity, and alignment fashion are similar, regardless of resolution or Reynolds number.

Probability distribution functions (PDFs) of helicity [Fig. 1(a)] are compared to PDFs of other quadratic quantities such as dissipation and enstrophy. Helicity and other quantities are normalized by their rms values or mean values. The PDF of helicity has a longer tail compared to the Gaussian distribution, but helicity is less intermittent than enstrophy or dissipation. This comparison is consistent with the previous studies [28,38,39] about the intermittencies of strain rate, vorticity magnitude, local enstrophy, and local dissipation.

^{*}Present address: Division of Industrial Mathematics, National Institute for Mathematical Sciences, Daejeon 305-340, Korea.

[†]Corresponding author; clee@yonsei.ac.kr

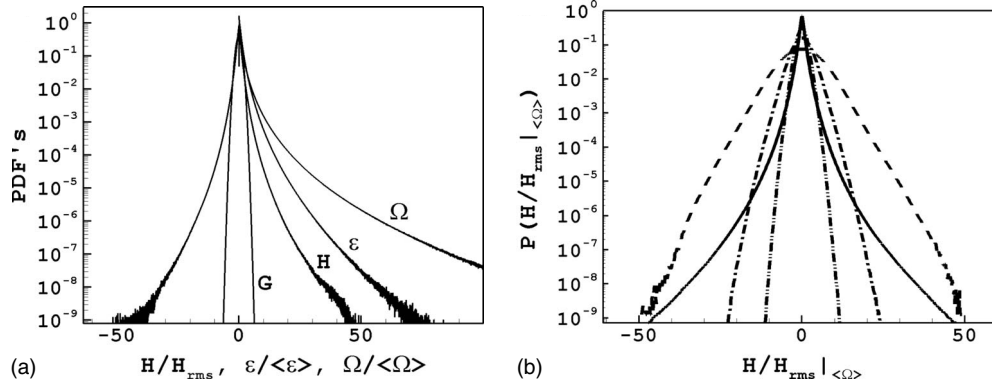


FIG. 1. Probability distributions of the helicity field. (a) PDFs of the Gaussian distribution, helicity (H/H_{rms}), dissipation ($\epsilon/\langle\epsilon\rangle$), and enstrophy ($\Omega/\langle\Omega\rangle$). (b) Conditional PDFs of helicity [$P(H/H_{rms}|\langle\Omega\rangle)$] normalized by the rms value of the total helicity field, conditioned by the following four different local enstrophy levels: $\langle\Omega\rangle \leq \Omega \leq 4\langle\Omega\rangle$ (dash-dot-dotted line), $4\langle\Omega\rangle \leq \Omega \leq 16\langle\Omega\rangle$ (dash-dotted line), $0 \leq \Omega < \infty$ (the total enstrophy field) (solid line), and $16\langle\Omega\rangle \leq \Omega \leq 64\langle\Omega\rangle$ (dashed line).

The conditional distributions of the helicity normalized by the rms value of the whole data set were investigated in terms of four different levels of local enstrophy [Fig. 1(b)]. Figure 1(b) presents statistical data relating to the intermittency of helicity with the following four different local enstrophy levels: $\langle\Omega\rangle \leq \Omega \leq 4\langle\Omega\rangle$, $4\langle\Omega\rangle \leq \Omega \leq 16\langle\Omega\rangle$, $16\langle\Omega\rangle \leq \Omega \leq 64\langle\Omega\rangle$, and $0 \leq \Omega < \infty$. Here, the quantity in brackets denotes mean value. Events in the range of $64\langle\Omega\rangle < \Omega < \infty$ are so rare, much less than a few percent, that most of the intense rotations are manifested in the events in the $16\langle\Omega\rangle \leq \Omega \leq 64\langle\Omega\rangle$ range of our calculation. The helicity field conditioned on $16\langle\Omega\rangle \leq \Omega \leq 64\langle\Omega\rangle$ seems to make the most substantial contribution to the long tail of total helicity, compared to those for other levels of enstrophy. From this, we can conclude that the intermittency of the spatial distribution of the helicity fields is closely related to the high enstrophy regions or intensely rotating structures.

This close relation between the intermittent distribution of helicity and high enstrophy is not surprising. It is evident probably from the definition of helicity that if vorticity is sufficiently high, then helicity is probably high as well. However, helicity is determined not only by the magnitude of vorticity, but also by the angle between velocity and vorticity. Thus, Fig. 1(b) provides the first clue that most intermittent distributions of helicity are intimately related to the dis-

tribution pattern of helicity on the highly rotating structures. Before investigating the behavior of angles in association with the rotational structures, we examine the correlations between helicity, enstrophy, and dissipation.

The correlation between dissipation and enstrophy was investigated due to the similar but different scaling exponents of enstrophy and dissipation in low Reynolds turbulent flows [39–42]. Furthermore, enstrophy and dissipation are closely related to the intermittency of acceleration [28–30]. Based on measurements of the velocity gradient tensors at fixed points, Zeff *et al.* [28] suggested a typical sequence in which rapid strain increasing comes first, followed by vorticity rising, and finally the strain experiences a sudden decline. Lee *et al.* [29] and Lee and Lee [30] showed that the source of the intermittency of acceleration of fluid turbulence is located around the edges of the vortical structures and the peak of acceleration is found between the regions dominated by enstrophy and dissipation.

Observations (Fig. 2) of correlations between helicity and enstrophy and between helicity and dissipation indicate the following: high values of helicity are always accompanied by high values of enstrophy. However, there is not a remarkable correlation between helicity and dissipation. This observation suggests that helicity has a more pronounced correlation with local enstrophy than with local dissipation. Figure

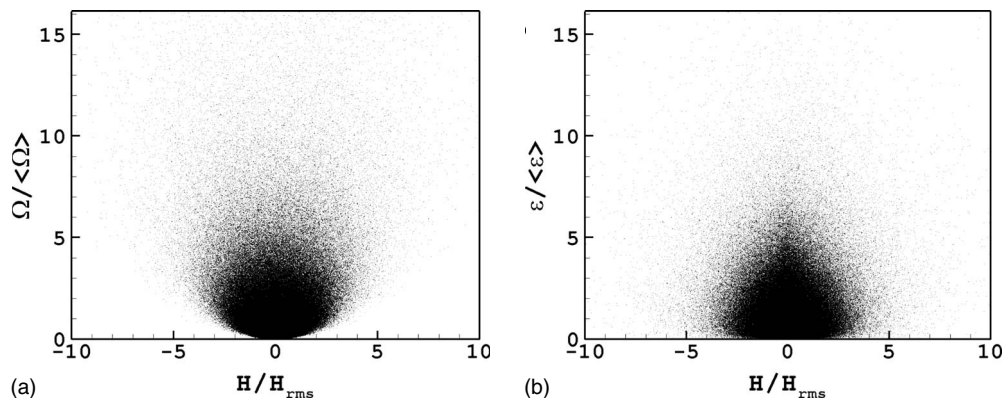


FIG. 2. Correlation between helicity, enstrophy, and dissipation. (a) Enstrophy vs helicity. (b) Dissipation vs helicity.

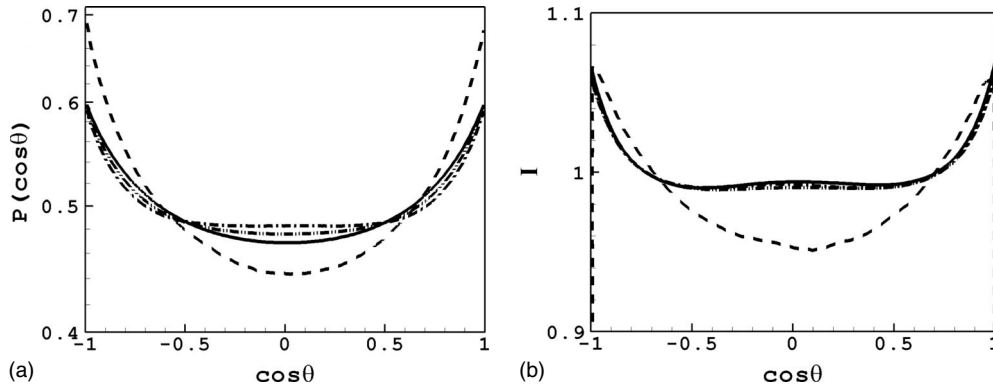


FIG. 3. Statistics of the helicity fields conditioned on four different enstrophy levels. (a) PDF of the relative helicity fields. (b) Distributions of the normalized helicity fields. Line legends are the same as in Fig. 1.

2(a) shows that for a given value of local helicity, the local enstrophy seems to have a lower bound since when local enstrophy vanishes, local helicity cannot have a finite value. However, for a non-small helicity, the local dissipation can vanish, which is possible near the core of vortical structures where the velocity field is almost solid-body rotation.

For a more detailed characterization of helicity in relation to vortical structures, we carried out two kinds of numerical experiments. The first observed quantity is relative helicity, defined by $\cos\theta = \mathbf{u} \cdot \boldsymbol{\omega} / |\mathbf{u}| |\boldsymbol{\omega}|$. The relative helicity field, $\cos\theta$, should be distinguished from the helicity fields, $\mathbf{u} \cdot \boldsymbol{\omega}$. Relative helicity is irrelevant to the magnitudes of velocity and vorticity and is only related to the directions of the interactions between the velocity and vorticity vectors. Relative helicity can be understood as, on average, the tendency of the alignment between the velocity and vorticity vectors. This matter has been discussed for various flows such as homogeneous and isotropic turbulence [19,21,43,44], the Taylor-Green vortex [20,22], channel flows [20,21], rotational flow [45], and the boundary and mixing layers [46].

Here, we investigated the relative helicity in terms of conditioned enstrophy levels. Figure 3(a) shows that events with θ close to 0° or 180° are more probable and more prominent in the case conditioned on $16\langle\Omega\rangle \leq \Omega \leq 64\langle\Omega\rangle$. This observation indicates that alignment is remarkably prominent in the region where rotation is strong, which corresponds to the core region of a vortex tube.

In the second experiment, which was conducted to identify the correlation between helicity and enstrophy, a new quantity defined by $I = \langle \mathbf{u} \cdot \boldsymbol{\omega} \rangle / (\langle |\mathbf{u}| \rangle \langle |\boldsymbol{\omega}| \rangle \cos\theta)$ is investigated with the same conditions for enstrophy as used in the previous experiment. If there is no correlation at all between the two quantities, I will be uniform at 1. As illustrated in Fig. 3(b), the correlations between velocity and vorticity are remarkable in the events close to 0° or 180° , especially in the range of $16\langle\Omega\rangle \leq \Omega \leq 64\langle\Omega\rangle$.

For example, the alignment between the velocity and vorticity vectors, especially in high enstrophy regions, is shown in Fig. 4. Tubelike shapes in the cubic box are isosurfaces at $\Omega = 10\langle\Omega\rangle$. Color contours on the surface of the structures indicate the angles formed by the velocity and vorticity vectors, which are calculated from the relative helicity. As we approach the core region of the structure, enstrophy rapidly

increases and highly rotating motion is presented. At the same time, as presented in the previous discussion, the velocity and vorticity vectors tend to be parallel with each other. The inset shows the isosurface at $\Omega = 30\langle\Omega\rangle$, which comes from the enclosed region at $\Omega = 10\langle\Omega\rangle$, clearly confirming the dominant alignment trend.

By combining the results of both experiments on relative helicity and the correlation of I , we can summarize that high values of helicity usually occur on the intensely rotating structures and that velocity and vorticity in those regions tend to be aligned. The alignment of the velocity and vortic-

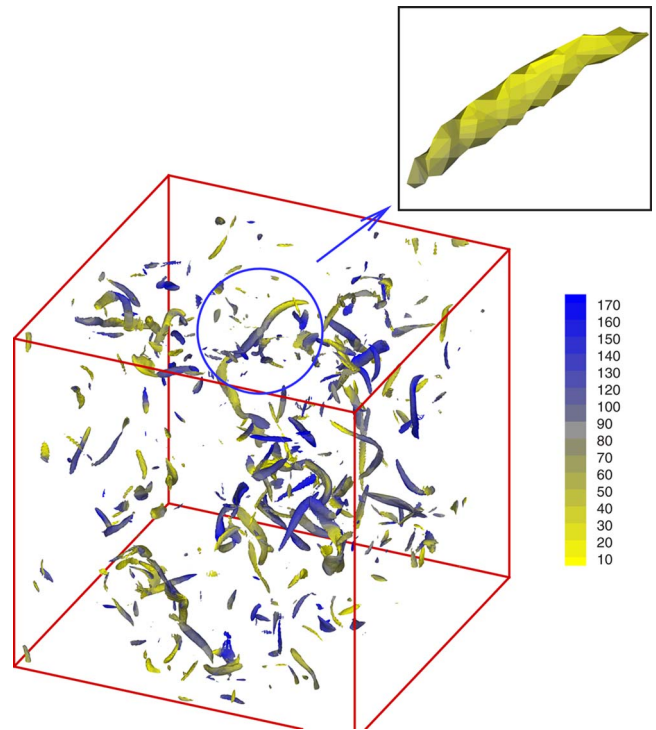


FIG. 4. (Color online) Isosurfaces of enstrophy at $\Omega = 10\langle\Omega\rangle$ and the colors on the surface denote the distribution of angles formed by the velocity and vorticity vectors. Inset presents the distributions of the angles on an isosurface of a high value of enstrophy, $\Omega = 30\langle\Omega\rangle$.

ity vectors on the intensely rotating structures is not a trivial event that can be suggested directly from the definition of local helicity.

On the other hand, an investigation of the statistics of velocity conditioned by the same levels of local enstrophy as in the previous experiment clearly shows that the distributions of velocity are almost the normal distribution regardless of conditional values of enstrophy. This indicates that velocity itself makes a smaller contribution to the alignment or intermittent nature of helicity.

In summary, the intermittency of helicity, which is a consequence of the complex behavior of the turbulent structures, is found to be intimately related to the coherent vortical structures, especially the highly rotating structures (Fig. 1). The highest enstrophy interval contributes most to the formation of the intermittency of helicity. Meanwhile, on

those structures, the velocity and vorticity vectors tend to be parallel, indicating that the nonlinear cascade to small scales is prohibited near the core of vortical structures, thus sustaining itself a little further. These observations of the correlations between helicity, dissipation, and enstrophy support the intimate relationship between helicity and enstrophy. Our finding of the trend between velocity and vorticity vectors in association with vortical structures will be useful for vortex identification [47,48] as well as for better understanding of the role of helicity in fluid turbulence.

We acknowledge support from the Korea Science and Engineering Foundation through Grant Nos. R01-2008-000-10664-0 and R31-2008-000-10049-0 (WCU Program). Most computations were carried out at KISTI Supercomputing Center.

-
- [1] H. K. Moffatt and A. Tsinber, *Annu. Rev. Fluid Mech.* **24**, 281 (1992).
- [2] A. Brissaud, U. Frisch, J. Leorat, M. Lesieur, and A. Mazure, *Phys. Fluids* **16**, 1366 (1973).
- [3] J. C. André and M. Lesieur, *J. Fluid Mech.* **81**, 187 (1977).
- [4] V. Borue and S. A. Orszag, *Phys. Rev. E* **55**, 7005 (1997).
- [5] L. Biferale, D. Pierotti, and F. Toschi, *Phys. Rev. E* **57**, R2515 (1998).
- [6] P. D. Ditlevsen and P. Giuliani, *Physica A* **280**, 69 (2000).
- [7] P. D. Ditlevsen and P. Giuliani, *Phys. Rev. E* **63**, 036304 (2001).
- [8] B. M. Koprov, V. M. Koprov, V. M. Ponomarev, and O. G. Chkhetiani, *Dokl. Phys.* **50**, 419 (2005).
- [9] Q. Chen, S. Chen, G. L. Eyink, and D. D. Holm, *Phys. Rev. Lett.* **90**, 214503 (2003).
- [10] Q. Chen, S. Chen, and G. L. Eyink, *Phys. Fluids* **15**, 361 (2003).
- [11] J. C. Bowman, C. R. Doering, B. Eckhardt, J. Davoudi, M. Roberts, and J. Schumacher, *Physica D* **218**, 1 (2006).
- [12] B. Galanti and A. Tsinober, *Phys. Lett. A* **352**, 141 (2006).
- [13] O. G. Chkhetiani and E. Golbraikh, *Phys. Lett. A* **372**, 5603 (2008).
- [14] A. Tsinober and E. Levich, *Phys. Lett.* **99A**, 321 (1983).
- [15] E. Levich and A. Tsinober, *Phys. Lett.* **93A**, 293 (1983).
- [16] A. K. M. F. Hussain, *J. Fluid Mech.* **173**, 303 (1986).
- [17] D. D. Holm and R. M. Kerr, *Phys. Fluids* **19**, 025101 (2007).
- [18] V. I. Arnold and B. A. Khesin, *Annu. Rev. Fluid Mech.* **24**, 145 (1992).
- [19] R. M. Kerr, *Phys. Rev. Lett.* **59**, 783 (1987).
- [20] R. B. Pelz, V. Yakhot, S. A. Orszag, L. Shtilman, and E. Levich, *Phys. Rev. Lett.* **54**, 2505 (1985).
- [21] M. M. Rogers and P. Moin, *Phys. Fluids* **30**, 2662 (1987).
- [22] L. Shtilman, E. Levich, S. A. Orszag, R. B. Pelz, and A. Tsinober, *Phys. Lett.* **113A**, 32 (1985).
- [23] L. Shtilman and W. Polifke, *Phys. Fluids A* **1**, 778 (1989).
- [24] L. Shtilman, *Phys. Fluids A* **4**, 197 (1992).
- [25] R. H. Kraichnan and R. Panda, *Phys. Fluids* **31**, 2395 (1988).
- [26] A. Tsinober, M. Ortenberg, and L. Shtilman, *Phys. Fluids* **11**, 2291 (1999).
- [27] A. V. Tur and E. Levich, *Fluid Dyn. Res.* **10**, 75 (1992).
- [28] B. W. Zeff, D. D. Lanterman, R. McAllister, R. Roy, E. Kostelich, and D. P. Latherop, *Nature (London)* **421**, 146 (2003).
- [29] C. Lee, K. Yeo, and J. I. Choi, *Phys. Rev. Lett.* **92**, 144502 (2004).
- [30] S. Lee and C. Lee, *Phys. Rev. E* **71**, 056310 (2005).
- [31] V. Eswaran and S. B. Pope, *Comput. Fluids* **16**, 257 (1988).
- [32] S. Chen, G. D. Doolen, R. H. Kraichnan, and Z.-S. She, *Phys. Fluids A* **5**, 458 (1993).
- [33] Z. S. She, S. Chen, G. Doolen, R. H. Kraichnan, and S. A. Orszag, *Phys. Rev. Lett.* **70**, 3251 (1993).
- [34] T. Gotoh, D. Fukayama, and T. Nakano, *Phys. Fluids* **14**, 1065 (2002).
- [35] L. Biferale, A. S. Lanotte, and F. Toschi, *Phys. Rev. Lett.* **92**, 094503 (2004).
- [36] T. Ishihara, Y. Kaneda, M. Yokokawa, K. Itakura, and A. Uno, *J. Fluid Mech.* **592**, 335 (2007).
- [37] D. A. Donzis, P. K. Yeung, and K. R. Sreenivasan, *Phys. Fluids* **20**, 045108 (2008).
- [38] R. M. Kerr, *J. Fluid Mech.* **153**, 31 (1985).
- [39] S. Chen, K. R. Sreenivasan, and M. Nelkin, *Phys. Rev. Lett.* **79**, 1253 (1997).
- [40] S. Chen, K. R. Sreenivasan, M. Nelkin, and N. Cao, *Phys. Rev. Lett.* **79**, 2253 (1997).
- [41] H. Chen, *Phys. Fluids* **10**, 312 (1998).
- [42] M. Nelkin, *Phys. Fluids* **11**, 2202 (1999).
- [43] R. B. Pelz, L. Shtilman, and A. Tsinober, *Phys. Fluids* **29**, 3506 (1986).
- [44] E. Kit, A. Tsinober, J. L. Balint, J. M. Wallace, and E. Levich, *Phys. Fluids* **30**, 3323 (1987).
- [45] P. Orlandi, *Phys. Fluids* **9**, 2045 (1997).
- [46] J. M. Wallace, J. Balint, and L. Ong, *Phys. Fluids A* **4**, 2013 (1992).
- [47] Y. Levy, D. Degani, and A. Seginer, *AIAA J.* **28**, 1347 (1990).
- [48] S. Zhang and D. Choudhury, *Phys. Fluids* **18**, 058104 (2006).